Analysis of Structure and function by the LysR-Type Transcriptional Regulator CbbR of Nostoc sp. PCC 7120

Hao-Xi Xu[1,2,3], Shu-Jing Han[1], Yong-Liang Jiang[1], Cong-Zhao Zhou[1]

[1] School of Life Sciences and Hefei National Laboratory for Physical Sciences at the Microscale, University of Science and Technology of China, Hefei, Anhui 230027, People's Republic of China.

[2] Department of Environmental and Chemical Engineering, Anhui Vocational and technical College, Hefei 230011, China.

[3] Corresponding author: Hao-Xi Xu (e-mail: haoxixu@163.com).

Acknowledgments

This work was supported by Natural Science Foundation of Anhui Provincial Education Department (No. KJ2019A0988) and Excellent Young Talents Fund Program of Higher Education Institutions of Anhui Province (No. GXFX2017213) and Excellent Young Talents Fund Program of Higher Education Institutions of Anhui Province (No. GXYQ2019178).

ABSTRACT The LysR-type Calvin–Benson–Bassham cycle transcriptional regulator CbbR plays an important role in CO_2 fixation in carbon metabolism in nature, which regulates the gene expression of the key enzyme RibisCO in the Calvin–Benson–Bassham (CBB) cycle. In this study, we optimized the conditions for the transformation, expression, and purification of CbbR in the model algae Nostoc sp. PCC 7120, obtained nick-DNA fragments that could tightly bind to CbbR_7120, and finally obtained CbbR protein crystals. These findings provide great assistance for the final crystallization of CbbR to solve the crystal structure of CbbR, and lay the foundation for understanding the mechanism of CO_2 fixation in the CBB cycle.

KEY WORDS Proteins, Crystals, Optimization

1 Introduction

Carbon metabolism is essential for the vital activities of various organisms. Organisms can adapt to different growth environments by delicately regulating the balance of carbon metabolism [1]. For most prokaryotes and eukaryotes, CO_2 is generally the only source of carbon [2]. Cyanobacteria are autotrophic photosynthetic microorganisms that have existed on earth since ancient times and are carbon-metabolism model microorganisms to study CO_2 as the carbon source [3]. Most cyanobacteria are aquatic organisms. To adapt to a gradually decreasing concentration of CO_2, cells have evolved to form a set of CO_2 concentration mechanisms (CCMs), which can facilitate the acquisition of inorganic carbon source materials (such as CO_2 and HCO_3^-) in cyanobacteria cells under extremely low CO_2 concentrations [4]. The inorganic carbon source is fixed by 1,5-ribulose diphosphate (RuBP) carboxylase/oxygenase (RibisCO) in the carboxysome by the transport system, which increases the CO_2 concentration in the active center of the enzyme [5][6]. In addition, extremely low concentrations of CO_2 molecules can also be reduced to carbohydrates in the Calvin–Benson–Bassham (CBB) cycle, thereby greatly improving the efficiency of photosynthesis [7].

The ultimate goal of the CBB cycle is to fix three molecules of CO_2 into one molecule of triose phosphoric acid, that is, the ingested CO_2 is reduced into the form of available carbon; therefore, these organisms can synthesize the macromolecular structure substances and energy substances essential for vital activities. In cyanobacteria, the uptake of inorganic carbon sources is greatly regulated at the transcription level. CCM-related genes can be induced by low carbon expression, and these genes are inhibited in high-concentration CO_2 environments [8]. The first step of CO_2 fixation in the CBB cycle is the reaction of CO_2 with RuBP into 3-phosphoglycerate (3-PGA) under the catalysis of ribulose-1,5-bisphosphate carboxylase oxygenase (RubisCO). The RibisCO-catalyzed reaction is the main pathway for the fixation of inorganic carbon, which is the key enzyme in the C3 pathway and is the center of various enzymes in the CBB cycle. However, due to a lack of high specificity and relatively low catalytic activity, O_2 and CO_2 will compete for the CO_2 binding site in RibisCO under aerobic conditions; thus, O_2 becomes linked to the carbohydrate chain to form the incorrect oxidation products [9]. Therefore, cells often increase the total amount of fixed inorganic carbon by synthesizing a large amount of RubisCO [10]. Moreover, because the assimilation of CO_2 has a relatively high energy demand and the burden of additional protein synthesis in cells, the transcriptional regulation of the RubisCo protein gene is of particular significance [11].

The Calvin–Benson–Bassham cycle transcriptional regulator CbbR regulates the gene expression of the key enzyme RibisCO in the CBB cycle [12]. The CbbR protein is a type of LysR-type transcriptional regulator (LTTR) [13]. CbbR-dependent regulation occurs in different types of organisms, including nonsulfur and purple sulfur bacteria, marine and freshwater chemical autotrophic bacteria, cyanobacteria, methylotrophic bacteria, and

different pseudomonas, mycobacteria, fusobacterium, etc. Currently, the spatial structure and function of the CbbR homologous proteins CcmR [14] and CmpR [15] have been partially resolved. These two transcription factors are both members of the LysR transcription factor family [16]. This family of proteins can regulate their own recognition of DNA sequences by binding with effector small molecules during the metabolic process [17]. However, the relevant structure and specific regulatory functions of CbbR, which is a key regulatory transcription factor that regulates CO_2 fixation, remain unclarified [18]. In the present study, we further analyzed the structure and function of CbbR in future studies by investigating and optimizing the expression, purification, and crystallization conditions of CbbR in model algae.

2 Materials and methods

2.1 Cloning, expression and purification

The coding region of full-length CbbR was amplified from the genomic DNA of Nostoc sp. PCC 7120 by PCR. The PCR product was cloned into a modified p28 vector with an N-terminal 6× His-tag (Table 1). The recombinant proteins were overexpressed in *Escherichia coli* strain Rosetta cells (DE3). Cells were cultured in LB culture medium (5 g of yeast extract, 10 g of NaCl, 10 g of tryptone per liter, pH 7) containing 16 μg/mL chloromycetin and 30 μg/mL kanamycin at 37°C until the $OD_{600\ nm}$ reached 0.8, and then the cells were induced with 0.2 mM isopropyl-β-1-thiogalactopyranoside (IPTG) for another 20 h at 16°C. The cells were harvested by centrifugation at 8 000 g for 4 min at 4°C and resuspended in loading buffer (20 mM Tris, 100 mM NaCl, pH 8.0). After sonication for 15 min and centrifugation at 16 000 g for 30 min at 4°C, the protein supernatant was loaded onto a nickel-nitrilotriacetic acid (Ni-NTA) column (GE Healthcare) containing 0.1 M Ni^{2+} and equilibrated with the same loading buffer. The Ni-NTA column was washed with equilibration buffer. The target protein was eluted with loading buffer containing 400 mM imidazole and then purified by gel filtration with a Superdex 200 column on the ÄKTAprime plus system (GE Healthcare) in binding buffer (20 mM Tris-Cl, pH 8.0, 1 M NaCl, 2 mM DTT, 0.1% β-OG). The purity of the target protein was confirmed by gel electrophoresis. The fractions containing the target protein were pooled and concentrated using a filter tube to a final concentration of 400 mM.

Table 1. Primer sequence information for the coding region of full-length CbbR from the genomic DNA of Nostoc sp. PCC 7120

CbbR_7120	Forward primer	5'-CAAAGCGATCGCCCGTGGCTTAGCACCACCACCACCA CCACTGA-3'
	Reverse primer	5'-GGGTTGTGAAGGCTACTACCGCCCATGGTATATCTCC TTCTT-3'

2.2 Electrophoretic mobility shift assay (EMSA)

EMSAs were performed with 5′-FAM-labeled double-stranded oligonucleotides (dsDNA). The complementary single-stranded oligonucleotides were synthesized by General Biosystems (Chuzhou, China) and annealed to produce double-stranded oligonucleotides. A 10 mL reaction volume containing a 5′-FAM-labeled probe was used with 2.5 μL of 5X binding buffer (100 mM HEPES pH 7.6, 5 mM EDTA, 50 mM $(NH_4)_2SO_4$, 5 mM DTT, 1% Tween 20, and 150 mM KCl per microliter) and suitable purified recombinant protein. The reaction lasted on ice for 15 min. When required, unlabeled competitors were added to the reaction system for another 15 min on ice. Then, the reaction solution containing protein-DNA complexes was loaded on 6% TBE-polyacrylamide gel with 0.5% TBE loading buffer on ice at 100 V for 2 h.

2.3 Crystallization

The full-length CbbR and protein-DNA complexes were applied for crystallization. Crystals were grown at 289 K using a Robot preliminary screen (hanging drop method) on 96-well plates with different conditions.

3 Results and discussion

3.1 Molecular sieve purification and electrophoresis verification of CbbR_7120

The CbbR protein in Nostoc sp. PCC 7120 model algae was selected. The optimal expression conditions (Table 2) were determined by detecting expression, followed by transformation, massive expression, protein purification and detection according to the optimal conditions.

Table 2. The optimal expression conditions of the CbbR protein in Nostoc sp. PCC 7120

Protein	Competent cells	T (°C)	Position	t (h)
CbbR_7120	Rosetta	16	Supernatant	20

(a)

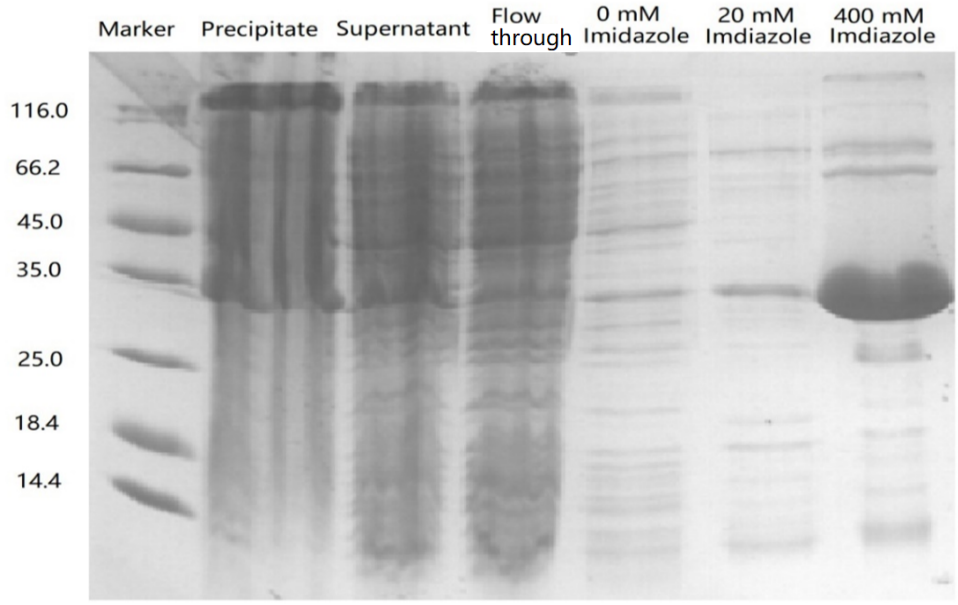

(b)

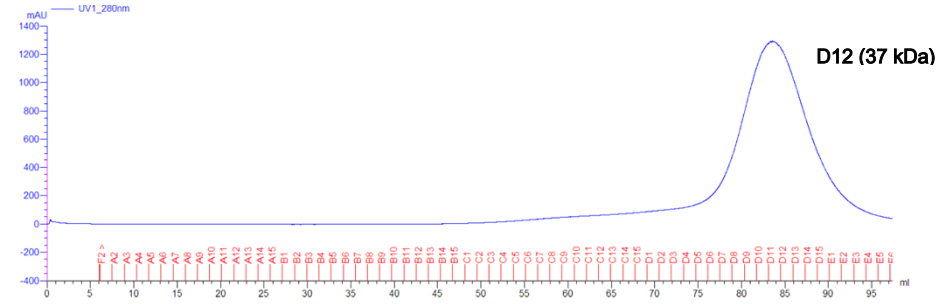

(c)

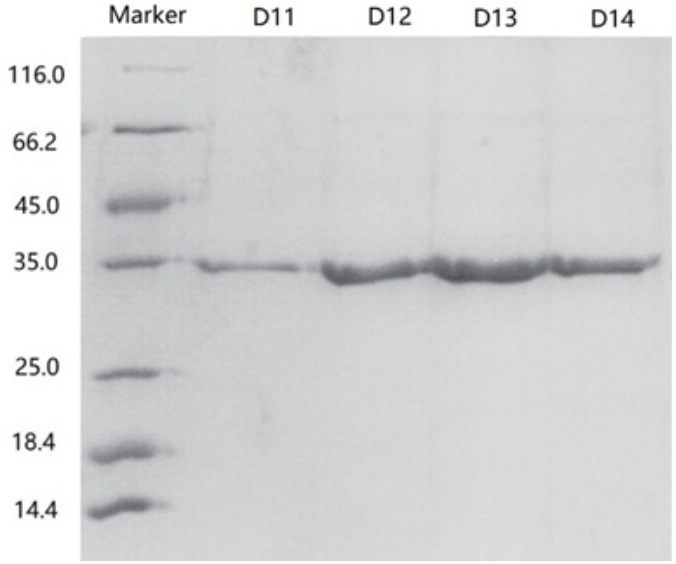

Figure 1. *(a)* Gel electrophoresis profile of protein fractions from centrifugation. *(b)* Gel filtration chromatography of the CbbR_7120 protein. *(c)* SDS-PAGE of the peak fractions from

gel filtration chromatography.

The protein CbbR_7120 was highly expressed (Fig. 1a). High yield protein bands were present when imidazole was eluted at a concentration of 400 mM but heteroproteins were also present. After purification by molecular sieve chromatography, CbbR_7120 peaked at location D12, and the peak was symmetric and uniform (Fig. 1b). High yield protein bands were present. Peak tip samples were taken for SDS-PAGE to verify protein purity, and we obtained high-purity protein samples (Fig. 1c).

3.2 Finding nick-DNAs by EMSA

The DNA sequence of rbcLXS from CbbR_7120 was estimated by the chip-seq method (Fig. 2). The FAM-tagged DNA sequence was designed based on the sequence in Table 3.

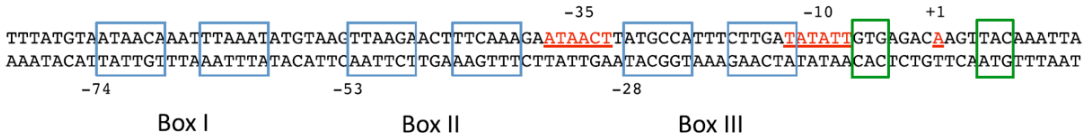

Figure 2. The DNA sequence of the rbcLXS promoter region [19]. The transcription initiation point of the operon (+1) and the −10 and −35 boxes are marked in red [20]. The three putative binding sites for All3953 (box I, box II and box III) are marked with blue boxes, and the NtcA-binding sites are marked with green boxes.

Table 3. The FAM tagged DNA sequence

Forward strand	**5'FAM**-TAATAACAAATTTAAATATGTAAGTTAAGAACTTTC AAAGAATAACTTATGCCATTTCTTGATAT-3'
Reverse strand	5'-ATATCAAGAAATGGCATAAGTTATTCTTTGAAAGTTCTT AACTTACATATTTAAATTTGTTATTA-3'

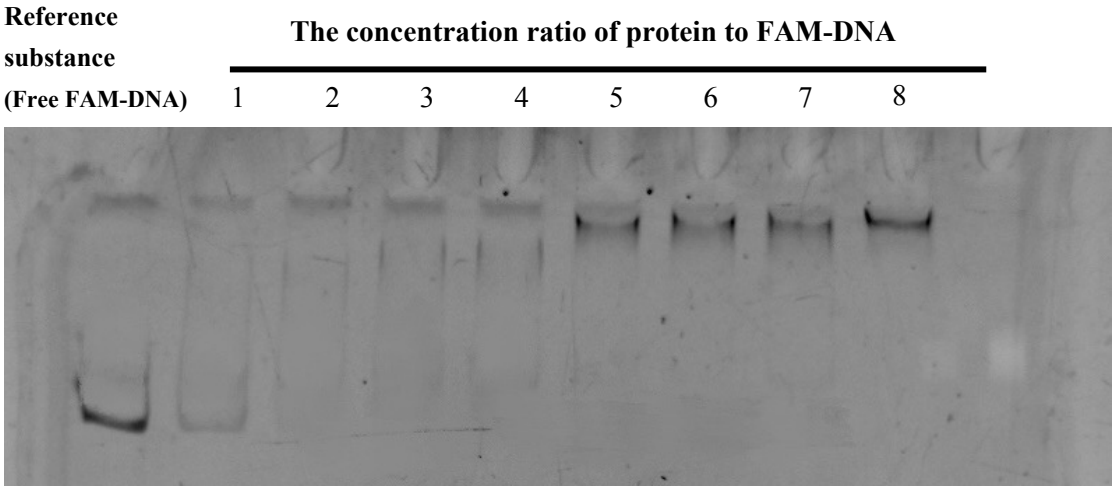

Figure 3. EMSA of the protein CbbR_7120 with different amounts of FAM-DNA for the minimum concentration ratio of protein-DNA-binding.

An amount ratio between protein and DNA equal to or greater than 5 indicates that the DNA and protein are completely bound. The concentration ratio between protein and DNA of 5 was therefore selected in the subsequent assay (Fig. 3).

Nick-DNA fragments（BOX 1, BOX2, BOX3） that could compete with FAM-tagged DNA were designed, including BOX I, BOX II, and BOX III (Table 4); that is, three binding sites that bound to the CbbR_7120 DBD domain. This assay was designed to prove whether the speculated binding sites were correct and to confirm the binding strength of different binding sites with CbbR_7120. The protein-bound FAM-DNA was free under complete competition.

Table 4. The designed competitive nick-DNA primer sequences

BOX 1	Forward primer	5’-TAATAACAAATTTAAATAT-3’
	Reverse primer	5’-ATATTTAAATTTGTTATTA-3’
BOX 2	Forward primer	5’-AGTTAAGAACTTTCAAAGA-3’
	Reverse primer	5’-TCTTTGAAAGTTCTTAACT-3’
BOX 3	Forward primer	5’-TTATGCCATTTCTTGATAT-3’
	Reverse primer	5’-ATATCAAGAAATGGCATAA-3’

(a)

Reference substance 1 (Free FAM-DNA)	Reference substance 2 (FAM-DNA -protein complexes)	The concentration ratio of competitive nick-DNA (BOX 1) to FAM-DNA							
		10	20	40	100	200	400	1000	2000

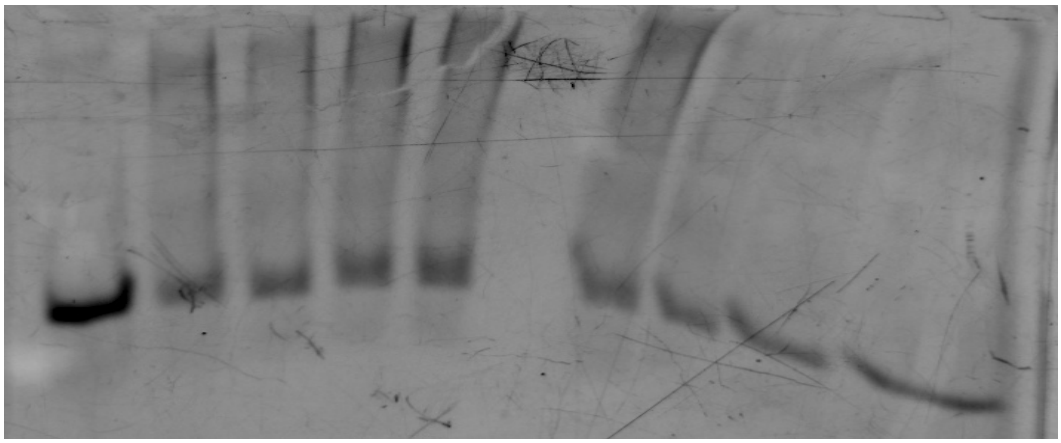

(b)

Reference substance 1 (Free FAM-DNA)	Reference substance 2 (FAM-DNA -protein complexes)	The concentration ratio of competitive nick-DNA (BOX 2) to FAM-DNA							
		10	20	40	100	200	400	1000	2000

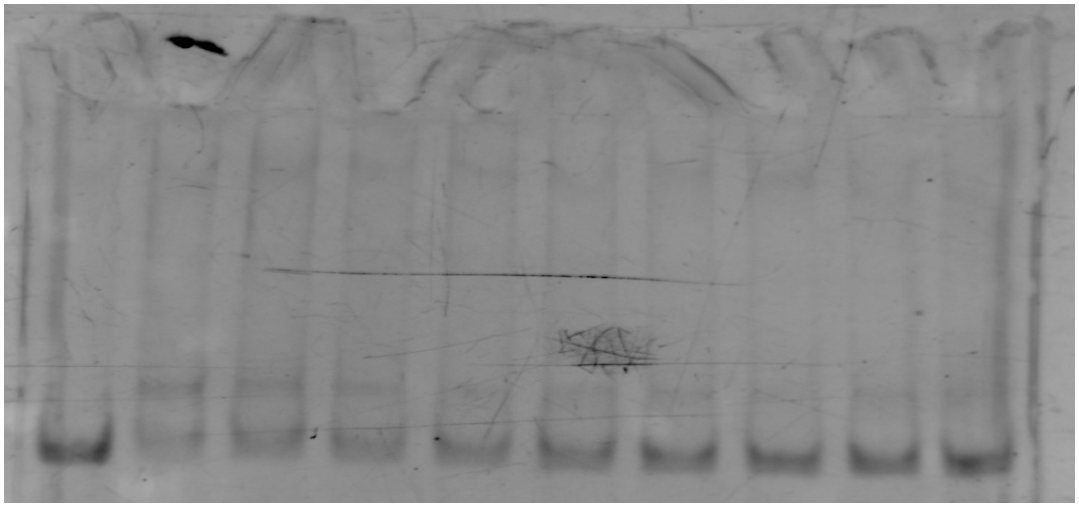

(c)

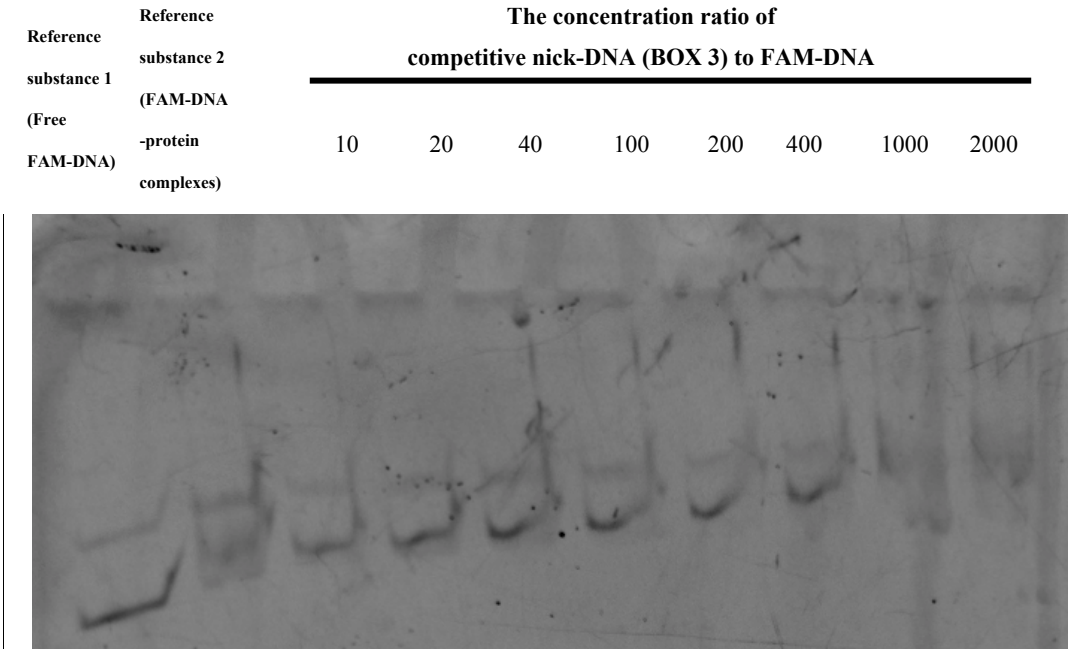

Figure 4. EMSA for detecting the protein binding ability of different competitive nick-DNAs with FAM-DNA.

When competitive nick-DNA (BOX 1) competitively bound to FAM-DNA (Fig. 4a), the concentration of free FAM-DNA fragments gradually increased, while the binding band gradually weakened. The ratio between competitive nick-DNA and FAM-DNA of 400 indicated that the protein-binding FAM-DNA was free and under complete competition.

When competitive nick-DNA (BOX 2) competitively bound to FAM-DNA (Fig. 4b), the concentration of the free FAM-DAN fragment did not significantly change due to competitive binding.

When competitive nick-DNA (BOX 3) competitively bound to FAM-DNA (Fig. 4c), the concentration of free FAM-DNA fragments gradually increased, while the binding band gradually weakened. The ratio between competitive nick-DNA and FAM-DNA of 1000 indicated that the protein-binding FAM-DNA was free and under complete competition.

Finally, it was confirmed that BOX 1 had the strongest binding ability to the CbbR_7120 protein; therefore, the seven nucleotide sequences in the linker region between BOX I and BOX II were optimized, different base-point mutations were designed from these optimal sequences, and the BOX I sequence was repeated and extended appropriately. Four optimal sequences (Box1OP1, Box1OP2, Box1OP3, Box1OP4) were formed (Table 5). Previous experiments have confirmed that the ability of BOX1OP1/BOX1OP3 to compete for binding proteins is relatively strong. Then, the concentration of competitive nick-DNA was decreased for comparison.

Table 5. Optimized competitive nick-DNA primer sequences

BOX1OP1	Forward strand	5'-TGTAATAACAAATTTAAATATGTCATATAACAAATTTAAATATGT-3'
	Reverse strand	5'-ACATATTTAAATTTGTTATATGACATATTTAAATTTGTTATTACA-3'
BOX1OP2	Forward strand	5'-TGTAATAACAAATTTAAATCTGTCAGATAACAAATTTAAATATGT-3'
	Reverse strand	5'-TGTATAAATTTAAACAATAGACTGTCTAAATTTAAACAATAATGT-3'
BOX1OP3	Forward strand	5'-TGTAATAACAAATTTAAATATTTAATATAACAAATTTAAATATGT-3'
	Reverse strand	5'-ACATATTTAAATTTGTTATATTAAATATTTAAATTTGTTATTACA-3'
BOX1OP4	Forward strand	5'-TGTAATAACAAATTTAAATATTTAATATAACAAATTTAAATATGT-3'
	Reverse strand	5'-ACATATTTAAATTTGTTATATTAAATATTTAAATTTGTT

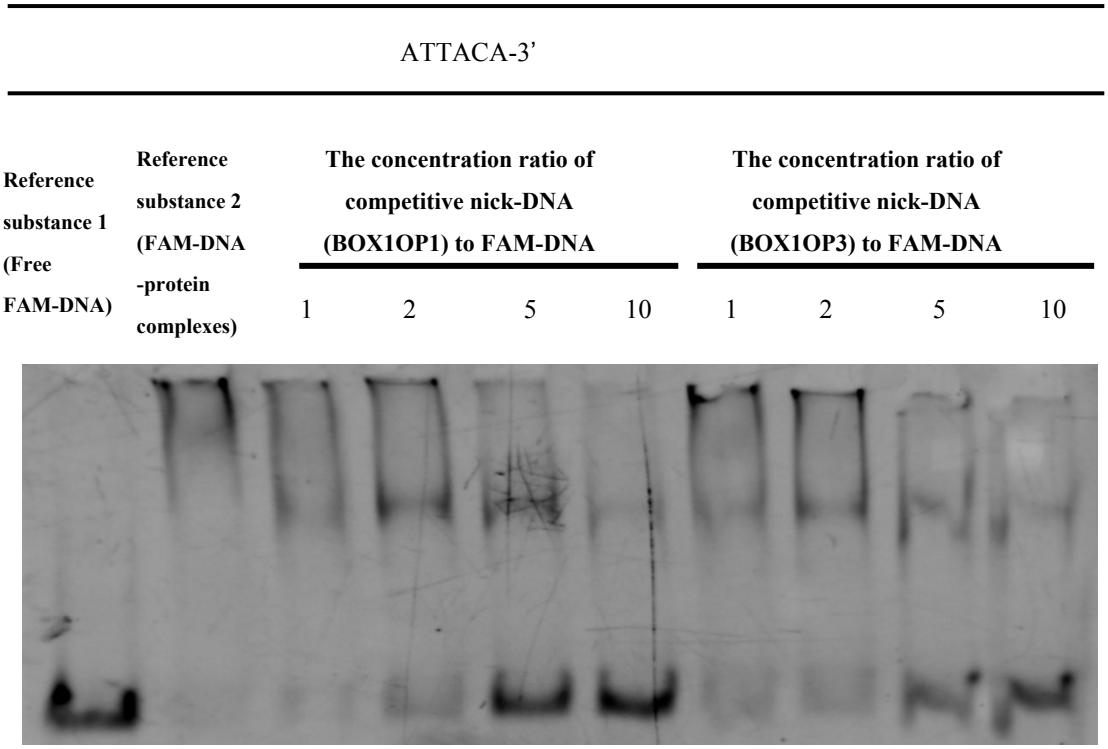

Figure 5. EMSA for detecting the protein binding ability of optimal competitive nick-DNAs with FAM-DNA.

When the ratio between added BOX1OP1 or BOX1OP3 and FAM-DNA concentration was 10, the binding bands of FAM-DNA with the protein generally were completely dissociated into free bands (Fig. 5). Both BOX1OP1 and BOX1OP3 had a strong binding affinity for the proteins; therefore, the two optimized fragments, BOX1OP1 and BOX1OP3, were used for the crystallization assay.

3.3 Crystallization

CbbR_7120 was crystallized separately and then coincubated with linker DNA overnight (Table 6).

Table 6. Crystallization Information

Linker_DNA	Conc. of Linker_DNA	Type of Pr.	Conc. of Pr.
BOX1OP1	220 mM	CbbR_7120	200 mM
BOX1OP3	220 mM	CbbR_7120	200 mM
-	-	CbbR_7120	400 mM

Microscopic observations revealed the precipitation of protein crystals under the following crystallization conditions (Fig. 6a).

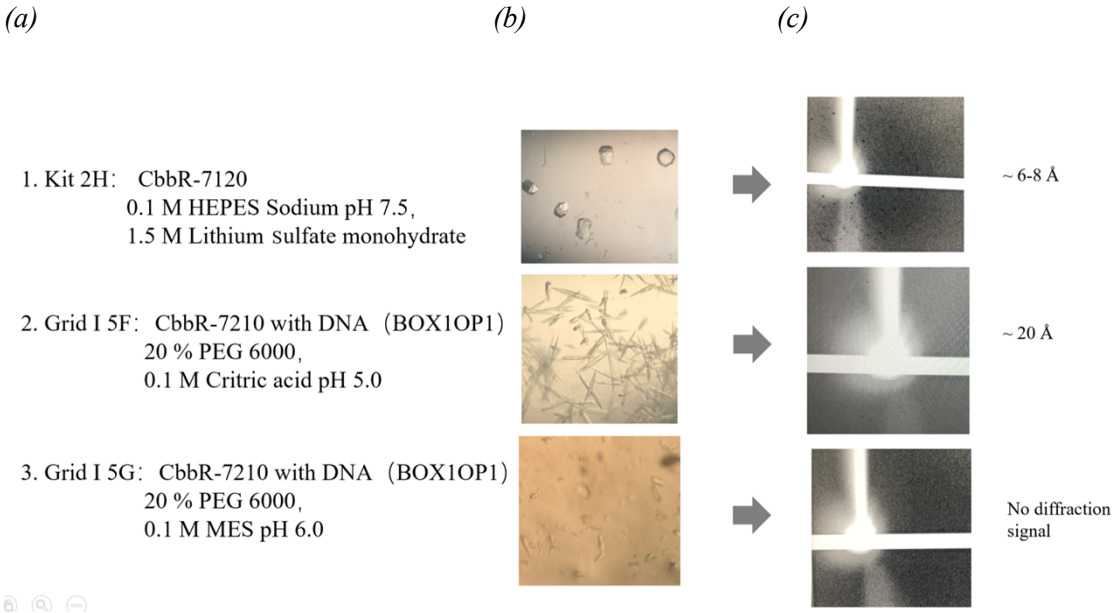

Figure 6. *(a)* Crystallization conditions. *(b)* Crystals of CbbR_7120 and CbbR_7120 with DNA. *(c)* X-ray diffraction patterns from the crystals.

In this study, we obtained the optimal expression conditions of CbbR in Nostoc sp. PCC 7120. The transformed, expressed and purified CbbR protein under the above conditions had high expression and relatively high purity. Additionally, an EMSA assay was used to obtain the DNA nick fragments that were tightly bound to the DBD region of CbbR_7120. Protein crystals were obtained by crystallization of the CbbR-7120, CbbR-7120 and DNA nick complexes. We optimized and analyzed the protein crystals and further elaborated their roles and functions in the CBB cycle in subsequent assays.

References

[1] Hügler M, Sievert SM. Beyond the Calvin cycle: autotrophic carbon fixation in the ocean. Annual review of marine science. 2011 Jan 15; 3:261-89.

[2] Teich R, Zauner S, Baurain D, Brinkmann H, Petersen J. Origin and distribution of Calvin cycle fructose and sedoheptulose bisphosphatases in plantae and complex algae: a single secondary origin of complex red plastids and subsequent propagation via tertiary endosymbioses. Protist. 2007 Jul 18;158(3):263-76.

[3] Badger MR, Bek EJ. Multiple Rubisco forms in proteobacteria: their functional significance in relation to CO_2 acquisition by the CBB cycle. Journal of experimental botany. 2008 May 1;59(7):1525-41.

[4] Price GD, Badger MR, Woodger FJ, Long BM. Advances in understanding the cyanobacterial CO_2-concentrating-mechanism (CCM): functional components, Ci transporters, diversity, genetic regulation and prospects for engineering into plants. Journal of experimental botany. 2008 May 1;59(7):1441-61.

[5] Terazono K, Hayashi NR, Igarashi Y. CbbR, a LysR-type transcriptional regulator from Hydrogenophilus thermoluteolus, binds two cbb promoter regions. FEMS microbiology letters. 2001 May 1;198(2):151-7.

[6] Dangel AW, Tabita FR. CbbR, the master regulator for microbial carbon dioxide fixation. Journal of bacteriology. 2015 Nov 15;197(22):3488-98.

[7] Dubbs JM, Bird TH, Bauer CE, Tabita FR. Interaction of CbbR and RegA* transcription regulators with the Rhodobacter sphaeroides cbb I promoter-operator region. Journal of Biological Chemistry. 2000 Jun 23;275(25):19224-30.

[8] Van Keulen G, Ridder AN, Dijkhuizen L, Meijer WG. Analysis of DNA binding and transcriptional activation by the LysR-type transcriptional regulator CbbR of Xanthobacter flavus. Journal of bacteriology. 2003 Feb 15;185(4):1245-52.

[9] Joshi GS, Zianni M, Bobst CE, Tabita FR. Further unraveling the regulatory twist by elucidating metabolic coinducer-mediated CbbR-cbbI promoter interactions in Rhodopseudomonas palustris CGA010. Journal of bacteriology. 2012 Mar 15;194(6):1350-60.

[10] Portis Jr AR, Li C, Wang D, Salvucci ME. Regulation of Rubisco activase and its interaction with Rubisco. Journal of experimental botany. 2008 May 1;59(7):1597-604.

[11] Dubbs JM, Tabita FR. Interactions of the cbbII promoter-operator region with CbbR and RegA (PrrA) regulators indicate distinct mechanisms to control expression of the two cbb operons of Rhodobacter sphaeroides. Journal of Biological Chemistry. 2003 May 2;278(18):16443-50.

[12] Van den Bergh, E R, Dijkhuizen, L, Meijer, W G. CbbR, a LysR-type transcriptional activator, is required for expression of the autotrophic CO_2 fixation enzymes of Xanthobacter flavus.[J]. Journal of Bacteriology, 175(19):6097-6104.

[13] Monferrer D, Tralau T, Kertesz MA, Dix I, Solà M, Usón I. Structural studies on the full-length LysR-type regulator TsaR from Comamonas testosteroni T-2 reveal a novel open conformation of the tetrameric LTTR fold. Molecular microbiology. 2010 Mar;75(5):1199-214.

[14] Woodger FJ, Bryant DA, Price GD. Transcriptional regulation of the CO_2-concentrating mechanism in a euryhaline, coastal marine cyanobacterium, Synechococcus sp. strain PCC 7002: role of NdhR/CcmR. Journal of Bacteriology. 2007 May 1;189(9):3335-47.

[15] Mahounga DM, Sun H, Jiang YL. Crystal structure of the effector-binding domain of Synechococcus elongatus CmpR in complex with ribulose 1, 5-bisphosphate. Acta Crystallographica Section F: Structural Biology Communications. 2018 Aug 1;74(8):506-11.

[16] Dangel AW, Luther A, Tabita FR. Amino acid residues of RegA important for interactions with the CbbR-DNA complex of Rhodobacter sphaeroides. Journal of bacteriology. 2014 Sep 1;196(17):3179-90.

[17] Omata T, Gohta S, Takahashi Y, Harano Y, Maeda SI. Involvement of a CbbR homolog in low CO_2-induced activation of the bicarbonate transporter operon in cyanobacteria. Journal of bacteriology. 2001 Mar 15;183(6):1891-8.

[18] Maddocks SE, Oyston PC. Structure and function of the LysR-type transcriptional regulator (LTTR) family proteins. Microbiology. 2008 Dec 1;154(12):3609-23.

[19] Picossi S, Flores E, Herrero A. The LysR-type transcription factor PacR is a global regulator of photosynthetic carbon assimilation in A nabaena. Environmental microbiology. 2015 Sep;17(9):3341-51.

[20] Nierzwicki-Bauer SA, Curtis SE, Haselkorn R. Cotranscription of genes encoding the small and large subunits of ribulose-1, 5-bisphosphate carboxylase in the cyanobacterium Anabaena 7120. Proceedings of the National Academy of Sciences. 1984 Oct 1;81(19):5961-5.

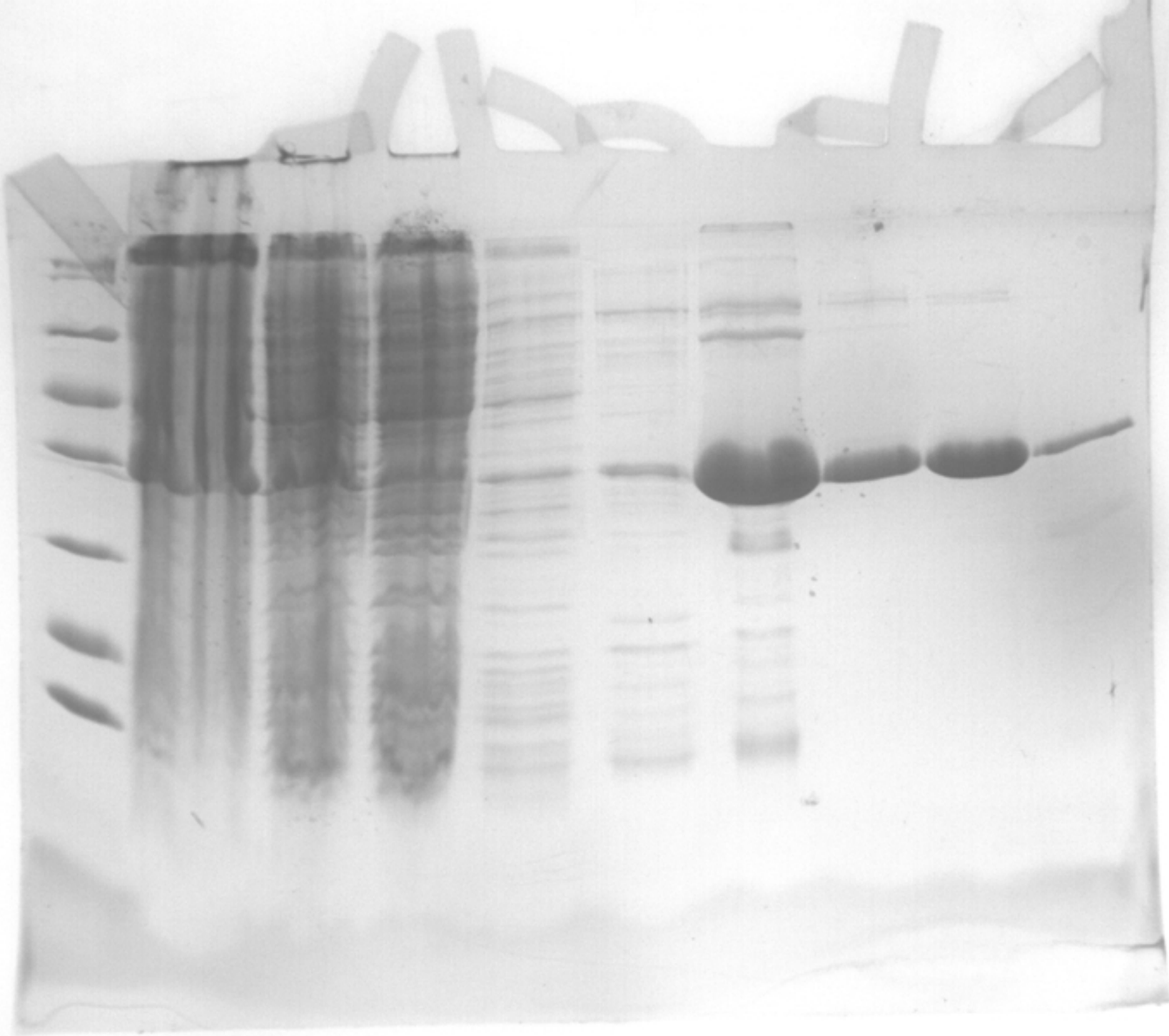

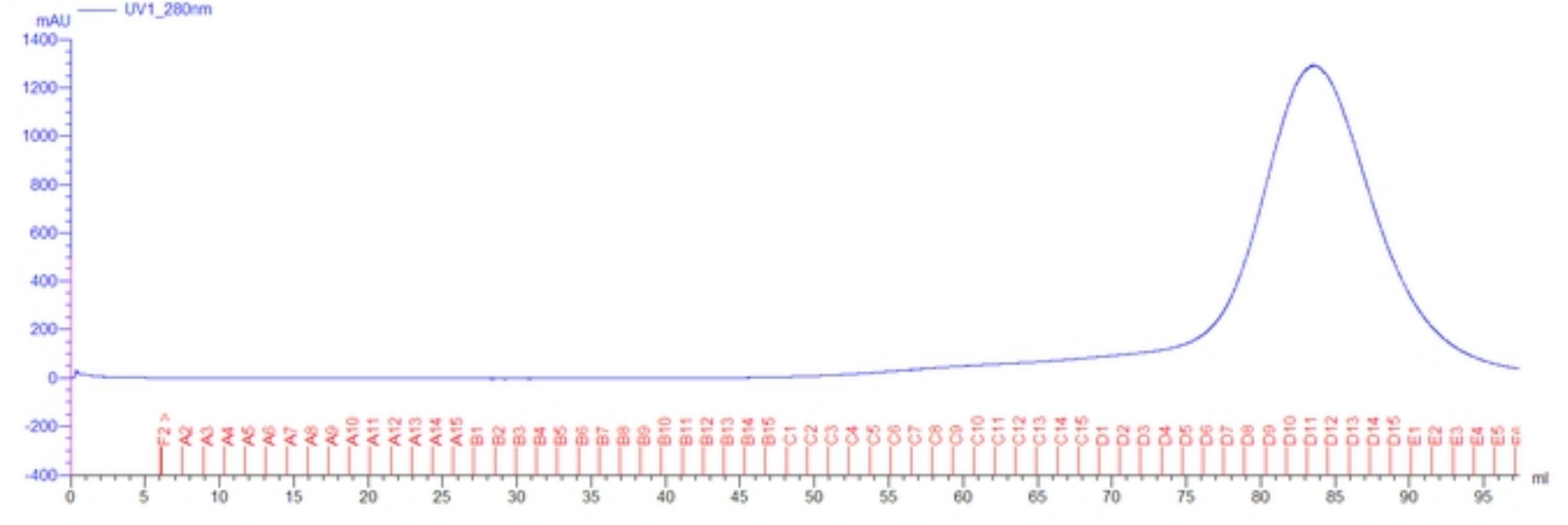
UV1_280nm
mAU
1400
1200
1000
800
600
400
200
0
-200
-400
F2 >
A2 A3 A4 A5 A6 A7 A8 A9 A10 A11 A12 A13 A14 A15
B1 B2 B3 B4 B5 B6 B7 B8 B9 B10 B11 B12 B13 B14 B15
C1 C2 C3 C4 C5 C6 C7 C8 C9 C10 C11 C12 C13 C14 C15
D1 D2 D3 D4 D5 D6 D7 D8 D9 D10 D11 D12 D13 D14 D15
E1 E2 E3 E4 E5
0 5 10 15 20 25 30 35 40 45 50 55 60 65 70 75 80 85 90 95
ml